Hydrology and Earth System Sciences, 8(1), *35–46* (2004) © EGU

Hydrology & Earth System Sciences

$^{234}U/^{238}U$ Disequilibrium along stylolitic discontinuities in deep Mesozoic limestone formations of the Eastern Paris basin: evidence for discrete uranium mobility over the last 1–2 million years

Pierre Deschamps[1,2], Claude Hillaire-Marcel[1], Jean-Luc Michelot[2], Régis Doucelance[3], Bassam Ghaleb[1] and Stéphane Buschaert[4]

[1]GEOTOP-UQAM-McGILL, P.O. Box 8888, Succ. Centre-Ville, Montréal, QC, Canada H3C 3P8

[2]CEREGE, Europôle méditerranéen de l'Arbois, BP 80 13 545 Aix-en-Provence, France

[3]Université Blaise Pascal, CNRS (UMR 6524), Observatoire de Physique du Globe de Clermont-Ferrand, 5 Rue Kessler, 63 038 Clermont-Ferrand Cedex, France

[4]ANDRA,1-7 rue Jean Monnet, 92298 Châtenay Malabry, France

Email for corresponding author: deschamps@cerege.fr

Abstract

The ($^{234}U/^{238}U$) equilibrium state of borehole core samples from the deep, low-permeability limestone formations surrounding the target argilite layer of the Meuse/Haute-Marne experimental site of the French agency for nuclear waste management -ANDRA- (Agence nationale pour la gestion des déchets radioactifs) was examined to improve understanding of naturally occurring radionuclide behaviour in such geological settings. Highly precise, accurate MC-ICP-MS measurements of the ($^{234}U/^{238}U$) activity ratio show that limestone samples characterised by pressure dissolution structures (stylolites or dissolution seams) display systematic ($^{234}U/^{238}U$) disequilibria, while the pristine carbonate samples remain in the secular equilibrium state. The systematic feature is observed throughout the zones marked by pressure dissolution structures: (i) the material within the seams shows a deficit of ^{234}U over ^{238}U (($^{234}U/^{238}U$) down to 0.80) and (ii) the surrounding carbonate matrix is characterised by an activity ratio greater than unity (up to 1.05). These results highlight a centimetric-scale uranium remobilisation in the limestone formations along these sub-horizontal seams. Although their nature and modalities are not fully understood, the driving processes responsible for these disequilibria were active during the last 1–2 Ma.

Keywords: uranium isotopes, multiple-collector ICP-MS, waste management, remobilisation, migration

Introduction

This study is part of geological investigations conducted since 1994 by ANDRA (Agence nationale pour la gestion des déchets radioactifs — the French agency for nuclear waste management) around the Underground Research Laboratory of Bure, excavated in a clay layer of the eastern part of the sedimentary Paris Basin, France (Fig. 1). ANDRA was given the responsibility of assessing the safety of high-level-radioactive waste (HLRW) repositories in deep geological environments. The safety of this method of nuclear waste disposal generally relies on a multi-barrier approach. Engineered and natural barriers are combined to prevent, or at least retard, radionuclide migration from the disposal site to the biosphere. These barriers must isolate wastes for periods sufficiently long to allow radioactivity to decay to acceptable levels. Although artificial barriers play an important role in long-term waste containment, the natural barrier (the host rock and the geological environment in which the repository is constructed, termed the 'far field'), plays a major role in the overall safety of the storage. In this framework, hydrological and geochemical behaviours of the potential host geological system must be taken into account in estimating its long-term confining capacities.

In this context, the systematics of naturally occurring

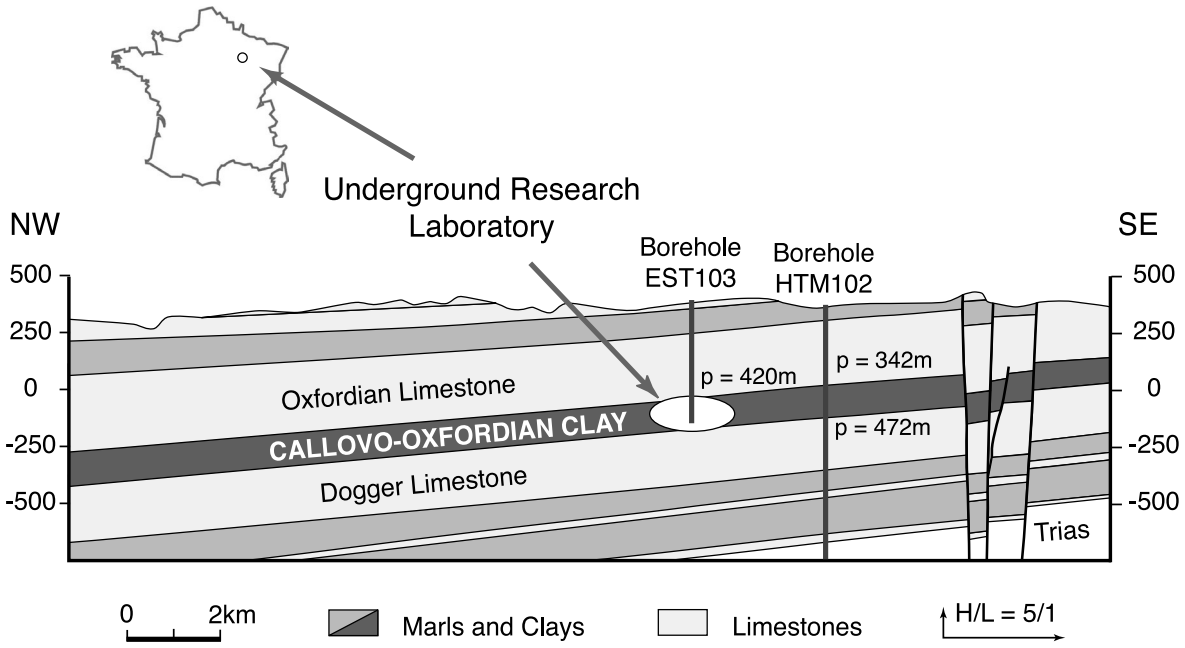

Figure III.1.: Location of the ANDRA Underground Research Laboratory (URL) in the eastern part of the Paris basin and Northwest/Southeast geological cross-section throughout the sedimentary target layers.

Fig. 1. *Location of the ANDRA Underground Research Laboratory (URL) in the eastern part of the Paris basin and Northwest/Southeast geological cross-section throughout the sedimentary target layers.*

uranium-decay series is a relevant tool which provides site-specific, natural chemical analogue information for the assessment, *in situ,* short-to-long-term migration of radionuclides in the far field of the repository (see review in Ivanovich, 1991; Ivanovich *et al*., 1992). One of the various applications of U-series systematics relevant to the study of radioactive waste disposal is the assessment of the chemical stability of potential host formations with respect to transporting chemical species by determination of the radioactive equilibrium state in the rock body (Schwarcz *et al*., 1982).

This study has examined the present state of equilibrium between ^{238}U and one of its daughters, ^{234}U, in sedimentary rocks at the ANDRA experimental site located in the eastern part of the Paris basin. Isotopic uranium analyses are reported of whole-rock samples from the deep, low-permeability limestone formations surrounding the target clayey layer. The highly precise and accurate MC-ICP-MS measurements of the ($^{234}U/^{238}U$) activity ratio highlight disequilibrium in the vicinity of pressure dissolution structures. This enables (i) the documentation of the *in situ* mobility of uranium within this sedimentary environment; and (ii) to deduce temporal indications on U-remobilisation in the system on a time scale of up to 1-2 Ma.

Principle of U-Th decay series study to radionuclide migration in rock matrix

Uranium and thorium are ubiquitous radioactive elements that occur naturally at trace levels in all Earth materials (Gascoyne, 1992). Their daughter nuclides are present in rocks in abundance, depending on: (i) their initial concentrations at the time of the system closure; (ii) the concentrations of their parents; and (iii) the time span elapsed since the last closure of the system. In a geological system that has remained closed to radionuclide migration for at least 1-2 Ma (i.e. a few half-lives of the longest-lived daughter of the U-Th series: ^{234}U, $T_{1/2}$ = 245 250 a), the activities (defined as disintegrations per minute per gram, or dpm g^{-1}) of the intermediate nuclides are equal to the activities of their parents. This state is known as secular equilibrium. Thus, for a host rock older than 2 Ma, the attainment of secular equilibrium in the U and Th series becomes a strong indicator of closed-system behaviour, although it is possible, but highly unlikely, that inward or outward fluxes of all radionuclides occur at an equal rate in an open system.

Conversely, when a departure from the state of equilibrium

between a parent and its daughter is observed, i.e. a daughter-parent activity ratio distinct from unity, the system has been disturbed by a process fractionating the two nuclides from each other (^{230}Th *vs* ^{234}U or ^{234}U versus ^{238}U, for example). This disruption from the secular equilibrium state originates from processes capable of fractionating nuclides from one another as a result of either their specific chemical properties or a phenomenon directly related to the radioactive decay itself, known as the recoil effect.

In low-temperature environments on the Earth's surface, discriminating chemical processes essentially occur at the water-rock interface and proceed from distinct properties of the radionuclides during water-rock interactions such as solubility, adsorption, complexation or redox-sensitive behaviour. For instance, uranium is more mobile than thorium during water-rock interaction, more particularly in oxidizing environments due to its high solubility in 6+ state, whereas, whetever the redox conditions, Th forms insoluble hydroxides. The uranium solubility is especially enhanced in the presence of carbonated water, where it may be complexed as uranyl carbonate ion.

The recoil effect is a general term referring to the different physical mechanisms related to radioactive decay and inducing disequilibrium among radionuclides[1]. After the radioactive decay of an α-emitting parent, the resulting daughter is emitted with a finite kinetic energy. The crystalline lattice where the parent was located is damaged and the recoil atom is displaced from this initial position. Depending on the authors, the distance of recoil displacement for the ^{238}U-^{234}Th couple varies between 10 nm and 70 nm (Andrews and Kay, 1983; Eyal and Olander, 1990; Fleischer, 2003; Kigoshi, 1971; Osmond and Ivanovich, 1992; Sun and Semkow, 1998). Two main mechanisms are usually invoked to account for subsequent fractionation. When the α-emitter parent is located close to the edge of the grain, the recoil atom can be ejected directly from the grain into an adjacent phase, in most cases, the interstitial liquid phase (Kigoshi, 1971). Alternatively, after the parent disintegration, the daughter is located in a radiation-damaged site within the mineral grain, where it is more prone to subsequent removal or chemical remobilisation by fluids, e.g. by oxidation (Fleischer, 1980; Fleischer and Raabe, 1978).

These two phenomena account more particularly for the universal ($^{234}U/^{238}U$) radioactive disequilibria observed in the hydrosphere where natural waters typically are enriched in ^{234}U (Osmond and Cowart, 1976, 1992; Osmond and Ivanovich, 1992). The two intermediate ^{234}Th and ^{234}Pa daughters between ^{238}U and ^{234}U are relatively immobile and have short half-lives (24.1 day and 1.18 minutes, respectively), so that their specific chemical behaviour cannot play a significant role in 238U-234U fractionation. Since the ^{234}U daughter has the same chemical behaviour as its ^{238}U parent, the direct recoil of ^{234}Th in solution and the recoil-induced vulnerability of ^{234}U to leaching are the only explanations for ($^{234}U/^{238}U$) disequilibria at the rock-water interface.

Regardless of the fractionating processes involved, the time scale in which this phenomenon occurs can be inferred directly from the half-lives of the radionuclides concerned. In the general case where the half-life of the daughter is shorter than that of its parent, as with the ^{234}U–^{238}U or ^{230}Th–^{234}U pairs, the time span required to return to equilibrium state is determined by the half-life of the daughter. Although ultimately the ability to assess a time scale is dependent on the analytical precision of the measurements, it is generally stated that the return to equilibrium occurs after 4–6 half-lives of the daughter (Bourdon *et al*., 2003; Condomines *et al*., 1988; Gascoyne *et al*., 2002). Therefore, U–Th series disequilibria are a sensitive tool to trace phenomena that have disturbed a given system and to constrain them chronologically by providing a wide range of time scales corresponding to the half-lives encountered in the ^{238}U, ^{235}U and ^{232}Th series.

The significance of these isotopic clocks to study radionuclide migration in deep geological formation was first addressed by Schwarcz *et al.* (1982). These authors discussed the chronological implications of radioactive disequilibrium observed on rock matrices. They focussed mainly on the ^{226}Ra, ^{230}Th and ^{234}U nuclides since their half-lives (1,599 a, 75,690 a and 245,250 a, respectively) are most appropriate to the time scale in which the migration of radionuclides in the far field must be assessed. This approach was then applied with success to deep experimental sites relevant to storage of radioactive waste, located in granitoid bedrock (e.g. Gascoyne and Cramer, 1987; Gascoyne and Schwarcz, 1986; Griffault *et al*., 1993; Smellie *et al.*, 1986; Smellie and Stuckless, 1985) or in volcanic tuff (Gascoyne *et al.*, 2002). In these studies, the primary focus was the altered and/or fractured zones of the rock matrix where water/rock interaction may have taken place preferentially. This approach permits investigation of the time scales of such interactions and, consequently, to constrain in time groundwater circulation events, since it is often understood that the two phenomena are related.

[1]For a more precise and exhaustive description of the recoil effect, refer to Gascoyne (1992), Ivanovich (1994) or Bourdon *et al.* (2003).

Geological setting and sampling

The French government authorised ANDRA to construct a scientific Underground Research Laboratory (URL) at a depth of 500 m in a 150-million-year-old clay formation in an area straddling the Meuse and Haute-Marne departments (eastern France).

The target formation belongs to Mesozoic sedimentary rocks in the eastern Paris Basin and is a thick (130 m), Callovo-Oxfordian argillite unit that is 420–550 m deep at the URL site (Fig. 2). This detrital clay-rich rock is composed of illite, ordered mixed-layered illite-smectite minerals dominated by illite, kaolinite, minor amounts of chlorite, and cemented by 25–30 wt % of micrite (ANDRA, 2001).

This formation is overlain and underlain by Oxfordian to Kimmeridgian and Bajocian/Bathonian (Dogger) limestones, respectively (Fig. 2.). These carbonate units display very low porosity (2–5%) and permeability, although some more porous (10–20%) metric scale levels located in the Oxfordian limestones are water productive. Sub-horizontal pressure dissolution structures are distributed throughout within these limestone formations (see Figs. 3 and 4). For the sake of simplicity, such structures will be referred to henceforth as 'stylolites', 'stylolitic seams' or 'stylolitised zones', although, they can actually be categorised either as 'stylolites', in the strict sense, or 'dissolution seams' according to the standard terminology proposed by Buxton and Sibley (1981) and Bathurst (1987).

At the regional scale, these stylolitic seams have been documented in all the Mesozoic limestone formations (Coulon, 1992). According to this author, they could have a tectonic origin and be related to the Oligocene extension in the western part of the Eurasian plate. However, some of them were probably formed earlier by overburden during sedimentary loading of the series (ANDRA, 2001).

The core samples analysed were obtained from the HTM 102 ANDRA prospecting borehole located near the site where the URL is being built. This 1100 m deep borehole was drilled throughout the whole sedimentary series from the Kimmeridgian to the Bathonian unit. It crosscuts the target Callovo-Oxfordian argillite unit found between 342.70 m and 472.16 m below core top.

Ten samples from the Bathonian and Oxfordian formations and two samples from the upper part of the Callovo-Oxfordian formation were examined. In the two limestone formations, sampling was mainly focused on zones displaying pressure dissolution structures. Seven of the ten limestone samples selected are characterised by sub-horizontal, millimetric to centimetric-scale seams. In these samples, the material inside the joints as well as parts of the surrounding carbonate matrix were subsampled (see Figs. 4 and 5). For the sampling of the material within stylolitic seams, care was taken to exclude as much of the surrounding matrix rock as possible.

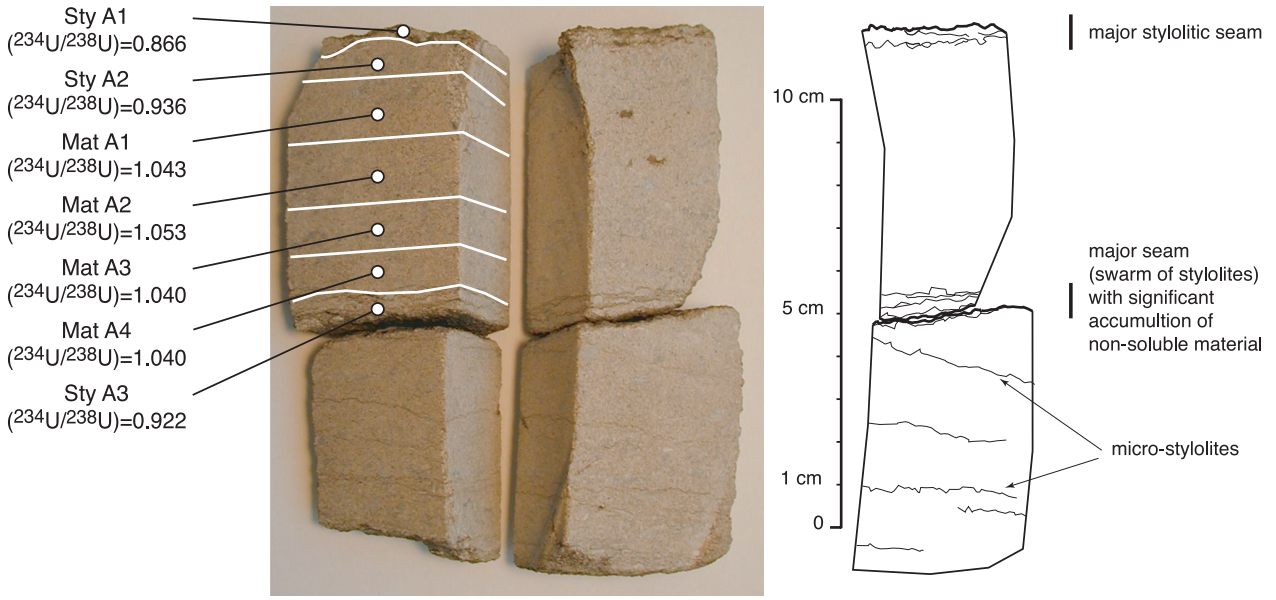

Fig. 2. *Subsampling of the HTM 02928 sample located in the Bathonian limestone formation (478 m depth). This sample is characterised by two major pressure dissolution structures (swarms of dissolution seams) that were sampled (Sty A1, Sty A2 and Sty A3 subsamples). The carbonate matrix located between these two stylolites was also sampled (Mat A1 to Mat A4 subsamples). The measured ($^{234}U/^{238}U$) activity ratio of these subsamples are reported. A schematic section of a plane surface of the sample highlights pressure-solution structures.*

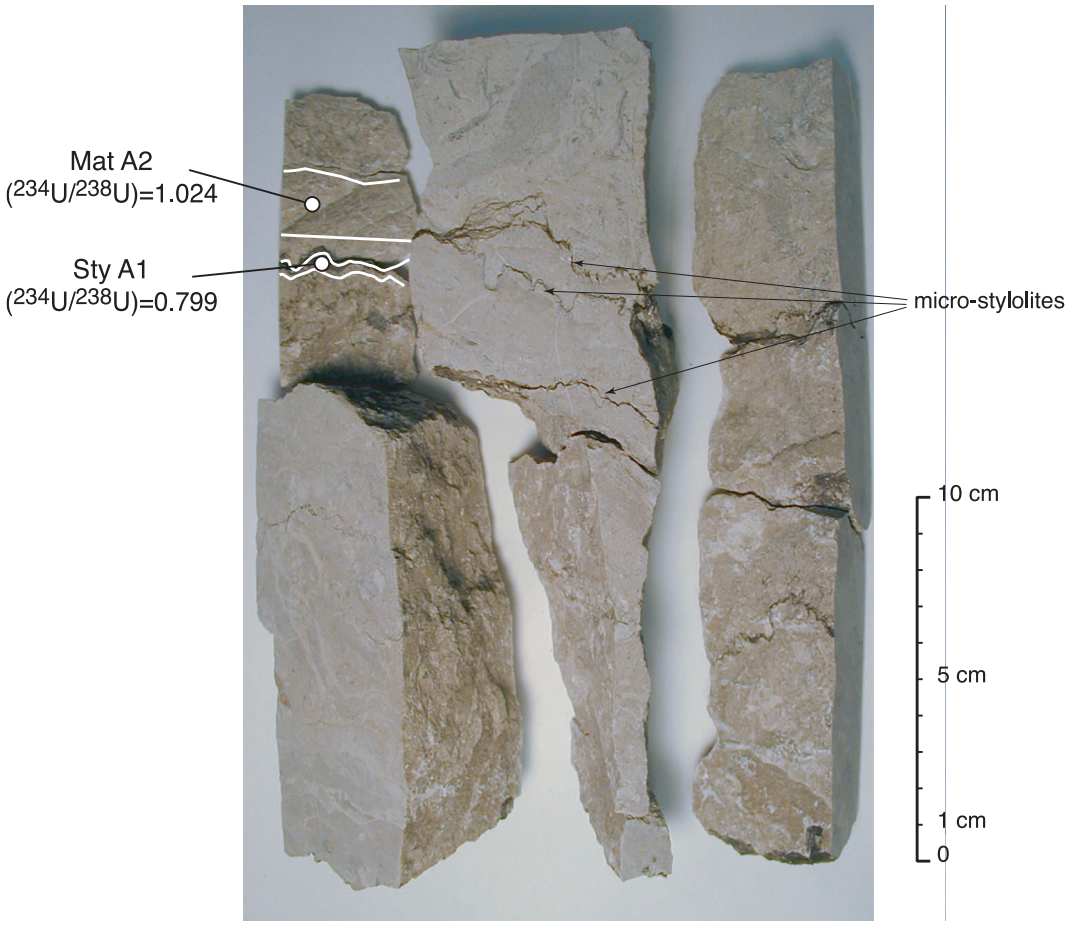

Fig. 3. Subsampling of the HTM 80824 sample located in the Oxfordian limestone formation (306 m depth). This sample is characterised by several sub-millimetric stylolitic seams. One of these seams (Sty A1 subsample), together with the embedding carbonate matrix within close proximity (Mat A1 subsample) was sampled. The measured ($^{234}U/^{238}U$) activity ratio is reported.

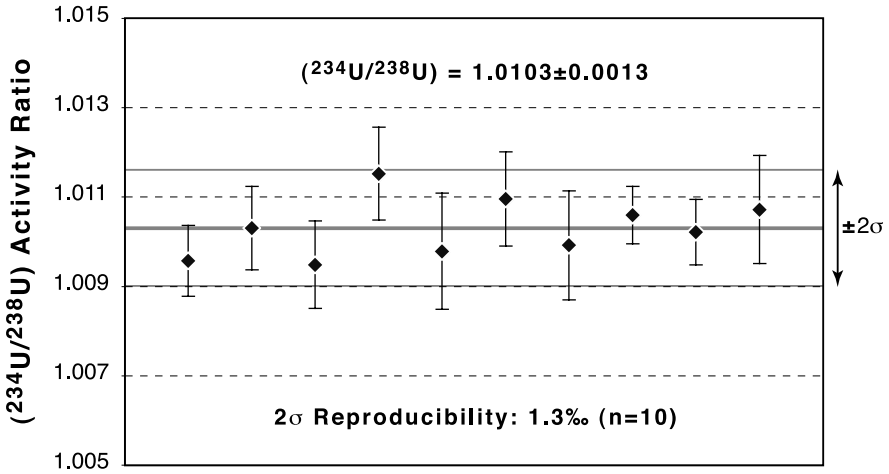

Fig. 4. *Replicate analyses of the ($^{234}U/^{238}U$) activity ratio of the HTM 02924 A #1 carbonate rock sample. The total external reproducibility is ±1.3‰†(2σ, n=10). Analyses were performed on a Micromass IsoProbe™MC-ICP-MS at the GEOTOP Research Center using the method described in Deschamps et al. (2003). ($^{234}U/^{238}U$) activity ratios are calculated using the half-life values determined by Cheng et al. (2000). Error bars indicate 2σ internal precision.*

Finally, five samples that are not characterised by pressure dissolution structures (and which will be referred to as 'pristine' samples hereafter) and 25 subsamples from stylolitised zones were crushed, finely powdered and analysed for their uranium content and $^{234}U/^{238}U$ isotopic composition.

Experimental techniques

CHEMICAL PROCEDURE

Because of the large amount of clay and organic impurities in the carbonate matrix, the chemical procedure for uranium separation and purification developed for these samples was modified from the usual chemical procedures used for pure carbonate matrices (Edwards *et al.*, 1987; Labonne and Hillaire-Marcel, 2000). More particularly, the digestion step needs to be adapted to ensure that the sample is totally dissolved.

Sample aliquots of 0.1 to 1 g were firstly weighed and burnt in a furnace at 650ºC for six hours to oxidise the organic matter. Secondly, aliquots were digested by sequential treatment with concentrated nitric acid and aqua regia in PFA Teflon Savillex™ previously spiked with a ^{236}U–^{233}U mixed solution (Deschamps *et al.*, 2003). The residues of insoluble material were centrifuged in nitric media, separated from the supernate liquid phase and further digested with concentrated nitric and hydrofluoric acids. At this step, the residues were totally dissolved. These solutions were dried before being dissolved in the previous supernate nitric solution. Uranium and thorium were then co-precipitated with Fe by the addition of ammonium hydroxide to pHs above 6 to 7 to optimise uranyl adsorption onto amorphous $Fe(OH)_3$ (Hsi and Langmuir, 1985; Waite *et al.*, 1994). Because of the large amount of clay in some samples, aluminum oxyhydroxides also co-precipitated with amorphous $Fe(OH)_3$. The mixture was centrifuged, the supernatant discarded and the precipitate was rinsed twice with Milli-Q water. The residue was then dissolved in 7N HNO_3, loaded onto a 2 ml column of anionic exchange resin (AG 1X8) and rinsed with 2 ml 7N HNO_3. Uranium and thorium fractions were then eluted together with MQ water and 6N HCl. This pre-purification step allows most of the major elements, especially Al, to be discarded. The fraction containing U and Th was dried down before being re-dissolved in 6N HCl. Uranium and thorium fractions were separated on a second 2 ml column of anionic exchange resin (AG 1X8). The Th fraction was eluted with 6N HCl, then dried before being purified on a 0.5 ml column of anionic exchange resin (AG 1X8) in 7N HNO_3. This Th fraction was stored for later analysis. The U fraction was eluted with MQ water, dried and purified on a 0.2 ml column of extraction chromatographic resin (U/Teva Elchrom™ in 2N HNO_3). The chemical yield for uranium achieved using this protocol was always greater than 90%.

MC-ICP-MS ANALYSES

The uranium analyses were performed on a Micromass IsoProbe™ MC-ICP-MS at the GEOTOP Research Center. In contrast to the methods usually carried out by other MC-ICP-MS users for uranium analyses (e.g. Luo *et al.*, 1997), Faraday detectors were used in static mode only. This approach avoids the problems of inter-calibration of the Daly and Faraday detector gains. However, since no Daly detector and its associated energy filter was used, the high abundance sensitivity of the instrument (up to 28 ppm) raises another major difficulty: that of precise estimation of tailing effects. A method for tail correction was developed, therefore, quite similar to that proposed by Thirlwall (2001), based on the effective and precise quantification of tail contribution underneath each peak due to adjacent ion beams, as determined independently by measurements of mono-isotopic ion beams.

For uranium analyses, mass discrimination bias is corrected for by the use of a ^{236}U–^{233}U double spike. Using an Aridus desolvating microconcentric nebuliser system, the amount of U consumed per $^{234}U/^{238}U$ analysis is about 200 ng, which is sufficient for obtaining a ^{234}U signal of 4 mV for 50 cycles of 5 seconds. The entire procedure is described in detail in Deschamps *et al.* (2003).

The accuracy and precision of the analytical protocol was assessed by measurements of a reference material (the NBL-112a standard, also called CRM-145, or formerly, NBS SRM-960). Nineteen replicate analyses of this standard yielded a mean $\delta^{234}U$ value of –36.42±0.80‰ (2σ) that is in excellent agreement with previously published values (see review in Deschamps *et al.*, 2003). For this specific study, the actual reproducibility on natural samples was determined by replicate measurements of an in-house carbonate standard, a powdered Bathonian limestone sample (HTM 02924 Mat #1) from the ANDRA HTM 102 borehole. The results, reported in Table 1 and Fig. 5, yielded a mean ($^{234}U/^{238}U$) activity ratio of 1.103±0.0013 (2σ, n= 10), which yields a total reproducibility (analytical plus chemical) of ~1.3‰, at the 95% confidence level. For the uranium concentration, a total reproducibility of 5‰ was obtained ([^{238}U] = 526.8±2.9 ppb, 2σ, n= 10).

Results

Uranium concentration and ($^{234}U/^{238}U$) activity ratio results

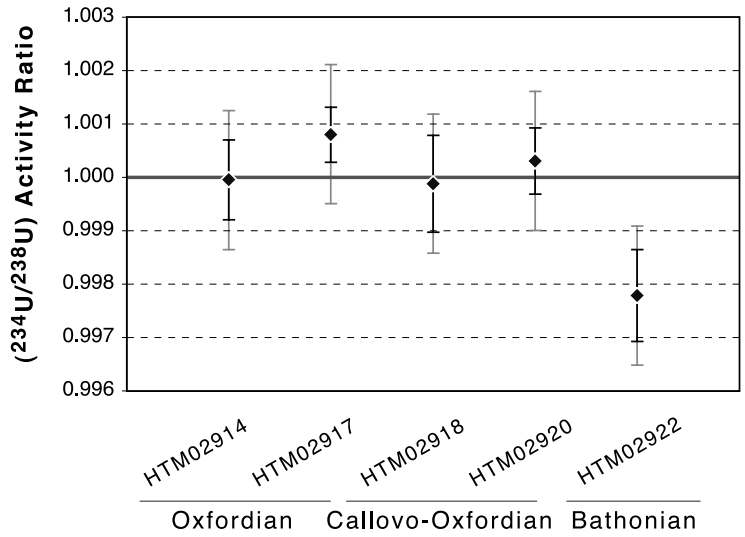

Fig. 5. *($^{234}U/^{238}U$) activity ratio measurements of pristine samples from the ANDRA HTM 102 borehole core. ($^{234}U/^{238}U$) activity ratios are calculated using the half-life values determined by Cheng et al. (2000). Error bars indicate either 2σ internal precision (black) or 2σ external precision (grey).*

Table 1. Replicate measurements of the ($^{234}U/^{238}U$) activity ratio and uranium content of an in-house limestone rock standard (HTM 02924 A #1 sample) with the GEOTOP MicroMass IsoProbe™ MC-ICP-MS.

Sub-Sample	^{238}U (ppb)	($^{234}U/^{238}U$) AR*
#1	526.736 ± 0.4	1.0096 ± 0.0008
#2	523.986 ± 0.5	1.0103 ± 0.0009
#3	527.906 ± 0.4	1.0095 ± 0.0010
#4	526.395 ± 0.4	1.0115 ± 0.0010
#5	528.397 ±0.5	1.0098 ± 0.0013
#6	528.422 ± 0.5	1.0110 ± 0.0011
#7	528.023 ± 0.5	1.0099 ± 0.0012
#8	525.280 ± 0.5	1.0106 ± 0.0006
#9	526.605 ± 0.5	1.0102 ± 0.0007
#10	526.294 ± 0.5	1.0107 ± 0.0012
Mean (± 2σ, n = 10)	**526.8** ± 2.9	**1.0103** ± 0.0013
2σ (%)	**0.55%**	**0.13%**

* ($^{234}U/^{238}U$) activity ratios (AR) are calculated using the half-life values given by Cheng *et al*. (2000).

All errors are given at the 95% confidence level (2σ).

of 30 samples, together with a brief description (host formation, depth, length and sample type — matrix versus seams) are listed in Table 2. The errors listed in Table 2 and reported in Figs 4 and 5 are given at the 95% confidence level and represent the internal error of each analysis.

In the Oxfordian limestone formation, the uranium concentrations of the carbonate matrix samples vary from 1.2 to 1.9 ppm. For stylolite samples, the U concentrations increase to 3.7–4.3 ppm. The same pattern is observed in the Bathonian formation: the carbonate matrix samples display between 0.2 and 0.6 ppm of U, whereas the stylolite samples show U-contents as high as 4 ppm. These data are within the range of uranium abundance typically encountered in such sedimentary rocks (Gascoyne, 1992).

($^{234}U/^{238}U$) results of the pristine samples, illustrated in Fig. 5, show near secular equilibrium values. This figure also shows, for each observation, the total analytical reproducibility achieved in the course of this study (1.3‰, 2σ). Figure 6 presents the ($^{234}U/^{238}U$) activity ratio of the stylolitised samples (surrounding carbonate matrix versus stylolite subsamples). Materials within the stylolitic joints are characterised by ($^{234}U/^{238}U$) activity ratio from 0.999 to 0.799, while the surrounding carbonate matrix samples exhibit activity ratios between 1.002 and 1.053.

Discussion

The pristine limestone samples display secular equilibrium between ^{234}U and ^{238}U (Fig. 5.) indicating that there has been no differential migration of ^{234}U relative to ^{238}U in these samples in recent time and, likely, no U mobility at all. Indeed, it would be very unlikely that an opening in the chemical system could occur without any detectable fractionation between ^{234}U and ^{238}U, since such a phenomenon necessarily involves water/rock interactions

Table 2. Analyses of the ($^{234}U/^{238}U$) activity ratio and uranium content in samples from the ANDRA HTM 102 borehole with a MicroMass IsoProbe™ MC-ICP-MS at the GEOTOP research Center.

Sample	*Unit*	*Depth (m)*		*Sub-Sample*	*Type*[#]	^{238}U *(ppb)*	$(^{234}U/^{238}U)$ *AR*[*]
		Top	*Bottom*				
Pristine Samples							
HTM 02914	Oxfordian	337.69	337.71			1638.7±0.2	1.0000±0.0008
HTM 02917	Oxfordian	340.30	340.66			1194.6±1.0	1.0008±0.0005
HTM 02918	Callovo-Oxfordian	345.72	346.03			657.8±0.6	0.9999±0.0009
HTM 02920	Callovo-Oxfordian	349.94	349.96			1407.4±1.2	1.0003±0.0006
HTM 02922	Bathonian	472.00	472.10			1876.2±1.5	0.9978±0.0009
Stylolitized Samples							
HTM 80824	Oxfordian	306.00	306.22	Mat A2	carbonate matrix1	503.6±1.5	1.0244±0.0003
				Sty A1	stylolitic material	3880.3±5.8	0.7991±0.0005
HTM 07325	Oxfordian	322.30	322.64	Mat A4	carbonate matrix	1881.5±1.8	1.0023±0.0003
				Sty A1	stylolitic material4	354.7±4.2	0.9932±0.0003
HTM 02601	Oxfordian	323.50	323.76	Mat A2	carbonate matrix1	439.0±1.4	1.0028±0.0004
				Sty A2	stylolitic material	3740.6±3.5	0.9989±0.0002
HTM 02924	Bathonian	472.81	472.96	A #1	carbonate matrix	526.9±2.9	1.0106±0.0013
				A #9	carbonate matrix	654.4±0.6	1.0441±0.0007
				A #10	carbonate matrix	557.3±0.5	1.0344±0.0009
				A #6a	stylolitic material	4082.4±4.2	0.9628±0.0005
				A #6b	stylolitic material	2196.4±2.2	0.9799±0.0005
HTM 02926	Bathonian	472.96	473.17	A #3	carbonate matrix	463.0±0.4	1.0198±0.0006
				A #23	carbonate matrix	388.5±0.4	1.0203±0.0010
				A #12	stylolitic material	618.2±0.9	0.9361±0.0021
				A #26	stylolitic material	559.0±0.5	0.9154±0.0008
HTM 07322	Bathonian	476.48	476.87	Mat A	carbonate matrix	774.9±0.7	1.0303±0.0005
				Sty A1	stylolitic material	1149.5±1.1	1.0106±0.0005
				Sty B2	stylolitic material	834.4±0.8	0.9532±0.0006
HTM 02928	Bathonian	477.66	477.77	Mat A1	carbonate matrix	260.7±0.2	1.0427±0.0010
				Mat A2	carbonate matrix	252.5±0.2	1.0532±0.0012
				Mat A3	carbonate matrix	262.1±0.2	1.0399±0.0011
				Mat A4	carbonate matrix	279.8±0.3	1.0402±0.0013
				Sty A1	stylolitic material	970.3±0.9	0.8665±0.0010
				Sty A2	stylolitic material	487.8±0.5	0.9364±0.0009
				Sty A3	stylolitic material	479.2±0.4	0.9224±0.0010

[#] Carbonate matrix material refers to the embedding matrix sample in the vicinity of the stylolitic seams.

[*] $(^{234}U/^{238}U)$ activity ratios (AR) are calculated using the half-life values given by Cheng *et al.* (2000). All errors are given at the 95% confidence level (2σ).

and migration via interstitial fluids. ($^{234}U/^{238}U$) disequilibria, resulting from water/rock interaction and recoil effects at the water/rock interface, display generally highly significant departures from unity in fluid phases and, to a lesser extent, in the solid matrix (Osmond and Cowart, 1992; Osmond and Ivanovich, 1992). Consequently, although it depends ultimately on the water/rock ratio, one can expect that the disequilibria inherited by the matrix rock from such a phenomenon should be detectable by the high analytical precision achieved with the MC-ICP-MS technique (~1‰).

Concerning the HTM 02922 Bathonian sample, the disequilibrium observed (($^{234}U/^{238}U$) = 0.9978±0.0013) is

significant at the 2σ level, whereas this is not the case at the 3σ level. If this disequilibrium is confirmed, it could be attributed directly to the presence in its vicinity of a stylolitised zone (sample HTM 02924), located 80 cm down, that shows significant disequilibrium (see below). Moreover, this sample was considered pristine at the macroscopic scale only. It is, therefore, possible that, barely visible sub-millimetric stylolitic joints could have been present.

All the stylolites and associated carbonate matrix subsamples display significant ($^{234}U/^{238}U$) disequilibria (see Fig. 6.). The following features are systematically observed throughout samples of this type. The material within the seams shows: (i) a higher abundance of uranium than in the embedding carbonate matrix; and (ii) a significant deficit of ^{234}U over ^{238}U (($^{234}U/^{238}U$) down to 0.80). In contrast, the surrounding matrix is systematically characterised by ($^{234}U/^{238}U$) activity ratios greater than unity, up to 1.05 (see Figs. 2, 3. and 6.). The higher U-content in stylolitic material than in the embedding matrix can be explained by the presence of U-rich, insoluble residue, which consists mainly of clay minerals, organic matter and detrital accessory minerals. In this discontinuity, the accumulation of non-carbonate minerals arises from the pressure dissolution of host carbonate rocks along the stylolite interface in response to overburden or tectonic stress (Tucker, 1990; Wanless, 1979).

This phenomenon is observed in both the Bathonian and Oxfordian samples. However, the intensity of these disequilibria seems to be less pronounced in the Oxfordian samples than in the Bathonian samples. For instance, the HTM 07325 and HTM 02601 samples from the Oxfordian limestone exhibit only slightly significant disequilibria either in the stylolite (($^{234}U/^{238}U$) = 0.9932 and 0.9989, respectively) or in the surrounding carbonate matrix (($^{234}U/^{238}U$) = 1.0022 and 1.0028, respectively).

Two conclusions can be drawn from these results at this stage.

Firstly, although it is currently impossible to specify whether the system has been subject to a continuous process or whether it has been disturbed by a short and sudden event (see the distinction in Scott *et al*., 1992), a phenomenon of uranium migration has occurred within the last 1–2 Ma. Secondly, this uranium remobilisation is associated directly with the presence of the pressure dissolution structure since the disequilibria observed are encountered only in samples within and within close proximity to such discontinuities.

Furthermore, the distribution of the uranium isotopes

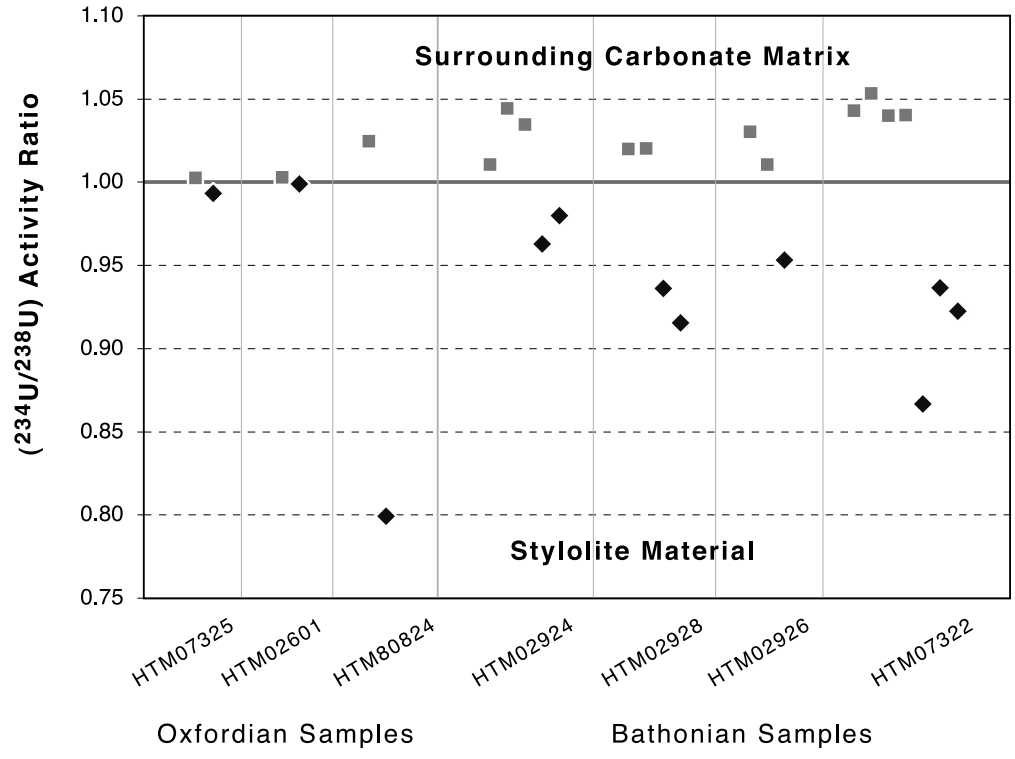

Fig. 6. *($^{234}U/^{238}U$) activity ratio measurements on stylolitic material (black diamonds) and embedding carbonate matrix (grey squares) samples from the ANDRA HTM 102 borehole core. ($^{234}U/^{238}U$) activity ratios are calculated using the half-life values determined by Cheng et al. (2000). Error bars are in the points.*

throughout the stylolitised zones suggests a relocation of uranium from the U-rich material within the seams into the surrounding U-low carbonate matrix. In this case, such a uranium transfer would be accompanied by an isotopic fractionation, the uranium remobilised from the stylolitic joint being characterised by a ($^{234}U/^{238}U$) activity ratio greater than unity.

The nature and the modality of the driving process(es) responsible for the remobilisation and fractionation of uranium are not understood and cannot be inferred solely from the ($^{234}U/^{238}U$) data presented here. However, two mechanisms can be evoked to explain the U-remobilisation observed: (1) late epidiagenetic processes associated with the presence of pressure dissolution structures, or (2) preferential fluid circulation along the stylolite pathway.

One cannot rule out totally that the uranium migration highlighted by ($^{234}U/^{238}U$) disequilibria is related, directly or indirectly, to the phenomenon of stylolitisation. The stylolitic discontinuities present high chemical and mineralogical heterogeneities due to the accumulation of non-soluble minerals. The ($^{234}U/^{238}U$) disequilibria observed in these zones may highlight geochemical transfers between the detrital material within the seams and the embedding carbonate matrix. Another possible explanation is an active stylolitisation or reactivation of this phenomenon in recent time (in the last 1–2Ma). Pressure dissolution processes, particularly in the horizontal plane, may result from overburden. One cannot, therefore, exclude that the current gravitational loading causes pressure dissolution and relocation of dissolved carbonate material within the embedding matrix. If this case arises, this would have important hydrological consequences since stylolitisation goes with reprecipitation of secondary carbonate phases within pore spaces of the host matrix, thereby reducing its porosity and permeability (Bathurst, 1975; Wanless, 1979). In both cases discussed above, the ($^{234}U/^{238}U$) disequilibria observed within stylolitic zones would characterise late diagenetic phenomena that do not involve massive transport of uranium into or out of the system and open system behaviour at large scale.

Stylolitic discontinuities could also constitute preferential conduits for flowing fluids (Dunnington, 1967). Fluids circulating through the stylolitic pathway could have remobilised uranium from the U-rich detrital material, infiltrated the surrounding matrix and subsequently redeposited it. Such a guess would imply an open dynamic system since it requires large-scale circulation of fluids to remobilise uranium. This second scenario would have major consequences on the conceptual modelling of the hydrological behaviour of the formations and, obviously, on the site performance assessment.

For the time being, the hypotheses advanced above remain highly speculative and can be considered only as working tracks. Complementary U–Th analyses are being carried out. More particularly, serial analyses performed perpendicularly to stylolitic surfaces should allow uranium migration within these zones to be characterised and, consequently, to specify the driving processes involved.

Conclusion

Although these results should be viewed as preliminary to a more exhaustive investigation of U-Series disequilibrium, some conclusions can already be drawn in regard to the problematic disposal of high level radioactive waste in the deep sedimentary formations around the Meuse/Haute-Marne Underground Research Laboratory of ANDRA.

These results provide *in situ* indications of the confining capacities of these deep sedimentary formations. Zones in Bathonian and Oxfordian limestones that do not show clear evidence for pressure-dissolution phenomena display ($^{234}U/^{238}U$) radioactive equilibrium, providing evidence for the current chemically closed system with respect to uranium.

Conversely, the ($^{234}U/^{238}U$) disequilibria observed in stylolitised zones highlight a discrete and recent migration of uranium in the limestone formations that underlie and overlay the clay target formation of the ANDRA Underground Research Laboratory. This is a major, surprising result since it is generally supposed that low-permeability limestone formations, such as those of the Meuse/Haute-Marne experimental site, have behaved as a chemically stable system after early diagenesis-related processes. Pressure dissolution structures play a major role in this remobilisation, but the nature and the modality of the processes responsible for these disequilibria are not well understood as yet. However, regardless of the processes involved, they have been active during at least the last 1–2 Ma. These last results are a significant contribution to the understanding of the dynamic behaviour of natural radionuclides in these Mesozoic series that can be considered as an analogue to the far field of potential disposals in clay layers. More particularly, they highlight that these pressure solution-related discontinuities are key structures that require further investigation.

Furthermore, methodological conclusions can be drawn from this study. The results highlight the importance of using highly precise and accurate techniques, such as MC-ICP-MS or TIMS. In fact, until now, most of the data published in this field were obtained by α-spectrometry. Their quoted analytical errors are commonly no better than 5% at the 95% level confidence for the ($^{234}U/^{238}U$) activity ratio (e.g. Gascoyne and Cramer, 1987; Gascoyne *et al.*, 2002;

Gascoyne and Schwarcz, 1986; Griffault *et al*., 1993; Latham and Schwarcz, 1987; Schwarcz *et al.*, 1982; Smellie *et al*., 1986; Smellie and Rosholt, 1984; Smellie and Stuckless, 1985). Since in most samples from this study the observed excess or deficit in ^{234}U *vs* ^{238}U does not exceed 5%, such disequilibria could not be highlighted by the current α-counting technique. Although, at this time, the MC-ICP-MS or TIMS techniques have not been fully exploited in this field, there is no doubt that they will open up new prospects.

Acknowledgements

The authors thank Dr. E. Pons-Branchu for constructive help and comments on the manuscript. PD is grateful to ANDRA for providing drill-core samples and PhD. financial support.

References

ANDRA, 2001. *Référentiel Géologique du Site Meuse-Haute Marne*. A RP ADS 99-005/B.

Andrews, J.N. and Kay, R.L.F., 1983. The U contents and $^{234}U/^{238}U$ activity ratios of dissolved uranium in groundwaters from some Triassic sandstones in England. *Chem. Geol.*, **41**, 101–117.

Bathurst, R.G.C., 1975. *Carbonate sediments and their diagenesis. Developments in sedimentology*. Elsevier, 658pp.

Bathurst, R.G.C., 1987. Diagenetically enhanced bedding in argillaceous platform limestones; stratified cementation and selective compaction. *Sedimentology*, **34**, 749–778.

Bourdon, B., Turner, S.P., Henderson, G.M. and Lundstrom, C.C., 2003. Introduction to U-series geochemistry. In: *Reviews in Mineralogy and Geochemistry*, B. Bourdon, G.M. Henderson, C.C. Lundstrom and S.P. Turner (Eds.), Uranium-Series Geochemistry. 1–21.

Buxton, T.M. and Sibley, D.F., 1981. Pressure solution features in a shallow buried limestone. *J. Sediment. Petrol.*, **51**, 19–26.

Cheng H., Edwards R.L., Hoff J., Gallup C.D., Richards D.A., and Asmerom Y., 2000. The half-lives of Uranium-234 and Thorium-230. *Chemical Geol.,***169**, 17–33.

Condomines, M., Hemond, C. and Allègre, C.J., 1988. U-Th-Ra radioactive disequilibria and magmatic processes. *Earth Planet. Sci. Lett.*, **90**, 243–262.

Coulon, M., 1992. La Distension Oligocène dans le nord-est du bassin de Paris (perturbation des directions d'extension et distribution des stylolites). *Bull. Société Géolog. France*, **163**, 531–540.

Deschamps, P., Doucelance, R., Ghaleb, B. and Michelot, J.L., 2003. Further investigations on optimized tail correction and high-precision measurement of Uranium isotopic ratios using Multi-Collector ICP-MS. *Chem. Geol.*, **201**, 141–160.

Dunnington, H.V., 1967. Aspects of diagenesis and shape change in stylolitic limestone reservoirs. *Proc.World Petroleum Congress*, **2**, 339–352.

Edwards, R.L., Chen, J.H. and Wasserburg, G.J., 1987. 238U-234U-230Th-232Th systematics and the precise measurement of time over the past 500,000 years. *Earth Planet. Sci. Lett.*, **81**, 175–192.

Eyal, Y. and Olander, D.R., 1990. Leaching of uranium and thorium from monazite; I, Initial leaching. *Geochim. Cosmochim. Acta*, **54**, 1867–1877.

Fleischer, R.L., 1980. Isotopic disequilibrium of uranium; alpha-recoil damage and preferential solution effects. *Science*, **207**, 979–981.

Fleischer, R.L., 2003. Etching of recoil tracks in solids. *Geochim. Cosmochim. Acta*, **67**, 4769–4774.

Fleischer, R.L. and Raabe, O.G., 1978. Recoiling alpha-emitting nuclei; mechanisms for uranium-series disequilibrium. *Geochim. Cosmochim. Acta*, **42**, 973–978.

Gascoyne, M., 1992. Geochemistry of the actinides and their daughters. In: *Uranium-series disequilibrium; applications to earth, marine, and environmental sciences,* M. Ivanovich and R.S. Harmon (Eds.). Clarendon Press, Oxford, UK. 34–61.

Gascoyne, M. and Cramer, J.J., 1987. History of actinide and minor element mobility in an Archean granitic batholith in Manitoba, Canada. *Appl. Geochem.*, **2**, 37–53.

Gascoyne, M. and Schwarcz, H.P., 1986. Radionuclide migration over recent geologic time in a granitic pluton. *Chem. Geol. Isotope Geoscience Section*, **59**, 75–85.

Gascoyne, M., Miller, N.H. and Neymark, L.A., 2002. Uranium-series disequilibrium in tuffs from Yucca Mountain, Nevada, as evidence of pore-fluid flow over the last million years. *Appl. Geochem.*, **17**, 781–792.

Griffault, L.Y., Gascoyne, M., Kamineni, C., Kerrich, R. and Vandergraaf, T.T., 1993. Actinide and Rare Earth Element characteristics of deep fracture zones in the Lac du Bonnet granitic batholith, Manitoba, Canada. *Geochim. Cosmochim. Acta*, **57**,1181–1202.

Hsi, C.K.D. and Langmuir, D., 1985. Adsorption of uranyl onto ferric oxyhydroxides; application of the surface complexation site-binding model. *Geochim. Cosmochim. Acta*, **49**, 1931–1941.

Ivanovich, M., 1991. Aspects of uranium/thorium series disequilibrium applications to radionuclide migration studies. *Radiochim. Acta*, **52/53**, 257–268.

Ivanovich, M., Latham, A.G., Longworth, G. and Gascoyne, M., 1992. Applications to radioactive waste disposal studies. In: *Uranium-series disequilibrium; applications to earth, marine, and environmental sciences,* M. Ivanovich and R.S. Harmon (Eds.). Clarendon Press, Oxford, UK. 583–630.

Kigoshi, K., 1971. Alpha-recoil thorium-234; dissolution into water and the uranium-234/uranium-238 disequilibrium in nature. *Science*, **173**, 47–48.

Labonne, M. and Hillaire-Marcel, C., 2000. Geochemical gradients within modern and fossil shells of Concholepas concholepas from Northern Chile: An insight into U-Th systematics and diagenetic/authigenic isotopic imprints in mollusk shells. *Geochim. Cosmochim. Acta*, **64**, 1523–1534.

Latham, A.G. and Schwarcz, H.P., 1987. The relative mobility of U, Th and Ra isotopes in the weathered zones of the Eye-Dashwa Lakes granite pluton, Northwestern Ontario, Canada. *Geochim. Cosmochim. Acta*, **51**, 2787–2793.

Luo, X., Rehkämper, M., Lee, D.C. and Halliday, A.N., 1997. High precision 230Th/232Th and 234U/238U measurements using energy-filtered ICP Magnetic Sector Multi-Collector mass spectrometry. *Int. J. Mass Spectrom. Ion Process.*, **171**, 105–117.

Osmond, J.K. and Cowart, J.B., 1976. The theory and uses of natural uranium isotopic variations in hydrology. *Atomic Energy Rev.*, 621–679.

Osmond, J.K. and Cowart, J.B., 1992. Ground water. In: *Uranium-series disequilibrium; applications to earth, marine, and environmental sciences,* M. Ivanovich and R.S. Harmon (Eds.) Clarendon Press, Oxford, UK. 290–333.

Osmond, J.K. and Ivanovich, M., 1992. Uranium-series mobilization and surface hydrology. IIn: *Uranium-series disequilibrium; applications to earth, marine, and environmental sciences,* M. Ivanovich and R.S. Harmon (Eds.) Clarendon Press, Oxford, UK. 259–289.

Schwarcz, H.P., Gascoyne, M. and Ford, D.C., 1982. Uranium-series disequilibrium studies of granitic rocks. *Chem. Geol.*, **36**, 87–102.

Scott, R.D., MacKenzie, A.B. and Alexander, W.R., 1992. The interpretation of ^{238}U-^{234}U-^{230}Th-^{226}Ra disequilibria produced by rock-water interactions. *J. Geochem. Exploration*, **45**, 345–363.

Smellie, J.A.T., Mackenzie, A.B. and Scott, R.D., 1986. An analogue validation study of natural radionuclide migration in crystalline rocks using uranium-series disequilibrium studies. *Chem. Geol.*, **55**, 233–254.

Smellie, J.A.T. and Rosholt, J.N., 1984. Radioactive disequilibria in mineralised fracture samples from two uranium occurrences in northern Sweden. *Lithos*, **17**, 215–225.

Smellie, J.A.T. and Stuckless, J.S., 1985. Element mobility studies of two drill-cores from the Goetemar Granite (Kraakemaala test site), Southeast Sweden. *Chem. Geol.*, **51**, 55–78.

Sun, H. and Semkow, T.M., 1998. Mobilization of thorium, radium and radon radionuclides in ground water by successive alpha-recoils. *J. Hydrol.*, **205**, 126–136.

Thirlwall, 2001. Inapropriate tail corrections can cause large inaccuracy in isotope ratio determination by MC-ICP-MS. *J. Anal. Atomic Spectrom.* **16**, 1121–1125.

Tucker, M., 1990. Diagenetic processes, products and environments. In: *Carbonate sedimentology,* M.E. Tucker and V.P. Wright (Eds.). Blackwell, Oxford, UK. 314–364.

Waite, T.D., Davis, J.A., Payne, T.E., Waychunas, G.A. and Xu, N., 1994. Uranium(VI) adsorption to ferrihydrite; application of a surface complexation model. *Geochim. Cosmochim. Acta*, **58**, 5465–5478.

Wanless, H.R., 1979. Limestone response to stress; pressure solution and dolomitization. *J. Sediment. Petrol.*, **49**, 437–462.